

# Numerical Modeling of the Arctic Ocean Ice System Response to Variations in the Atmospheric Circulation from 1948 to 2007

E. N. Golubeva<sup>a, b</sup> and G. A. Platov<sup>a</sup>

<sup>a</sup> *Institute of Numerical Mathematics and Mathematical Geophysics, Siberian Branch, Russian Academy of Sciences, pr. Akademika Lavrent'eva 6, Novosibirsk, 630090 Russia*

<sup>b</sup> *Novosibirsk State University, Novosibirsk, ul. Pirogova 2, 630090 Russia*

*e-mail: elen@ommfao.sccc.ru; plat@ommfao.sccc.ru*

Received June 17, 2008; in final form, August 8, 2008

**Abstract**—The results of model calculations aimed at reproducing climate changes in the Arctic Ocean due to variations in the atmospheric circulation are presented. The combined ocean–ice numerical model is based on NCAR/NCEP reanalysis data and its modified version of CIAF on the state of the lower atmosphere, radiative fluxes, and precipitation from 1948 to the present. The numerical experiments reveal the effect of the ice cover, water circulation, and thermohaline structure of the Arctic Ocean on variations in the state of the atmosphere. We found the heating and cooling periods in the Atlantic water layer, as well as the freshwater accumulation regimes in the Canadian Basin and freshwater flow through the Fram Strait and Canadian Archipelago straits. The numerical model reproduces a reconfiguration of the water circulation of the surface and intermediate layers of the ocean, a shift in the boundary between Atlantic and Pacific waters, and a significant reduction of the ice area.

**DOI:** 10.1134/S0001433809010095

## INTRODUCTION

Since the late 1980s, the Arctic Ocean has been characterized by significant warming and the enlargement of the Atlantic water layer [1–4], which is accompanied by a reduced sea-ice area and thickness [5–6]. An analysis of observational data has allowed researchers to believe that the Arctic Ocean is moving into a new and warmer state [7].

Numerical models of the ocean–ice–atmosphere interaction are powerful tools for investigating the physical aspects of local processes and identifying the main interrelations in a complex climate system [8]. Particularly, the results of model calculations on the basis of global models indicate that the Arctic is one of the regions most sensitive to climate changes [9].

Numerical models of the ocean considered separately from atmospheric models are unable to describe the ocean–atmosphere coupling; nevertheless, using data on oceanic surface currents, these models can be used to investigate the response of the ocean to variations in atmospheric effects. These investigations became possible as a result of processing of the NCEP/NCAR reanalysis database [10].

Throughout the past decade, the reproduction of climate changes in the Arctic Basin has been done on the basis of combined ocean–atmosphere models (for example, see [11–15]). The main aim of the international Arctic Ocean Model Intercomparison Project (AOMIP, [http://fish.cims.nyu.edu/project\\_aomip/overview.html](http://fish.cims.nyu.edu/project_aomip/overview.html)) is to develop advanced Arctic models that can

reproduce past events, reveal the interplay between climatic processes, and simulate the future state of the Arctic Ocean under different climate scenarios. Within a numerical experiment performed using the NCEP/NCAR reanalysis data for 1948 to the present, we have compared the results of calculations obtained by different models with observational data. We have matured parametrizations of physical processes and tested scientific hypotheses in the course of numerical experiments. Among the major lines of comparison, particular attention can be given to the research directions of this study: (a) studying the variability of circulation of Atlantic waters in the Arctic Basin; (b) revealing the mechanisms responsible for the accumulation of freshened water in the Canadian Basin and its flow into the northern Atlantic (see the schematic map of the area in Fig. 1); and (c) the numerical modeling of variations in the sea-ice thickness and area.

The aims of this study are

- (i) to reproduce the climate changes that occurred in the Arctic Ocean in the second half of the twentieth century and
- (ii) to reveal the interrelation between these changes and their dependence on the type of atmospheric circulation on the basis of a numerical ocean–ice model and of the NCEP/NCAR reanalysis database (and its modified version CIAF [16]) on the state of the lower atmosphere, radiative fluxes, and precipitation from 1948 to the present.

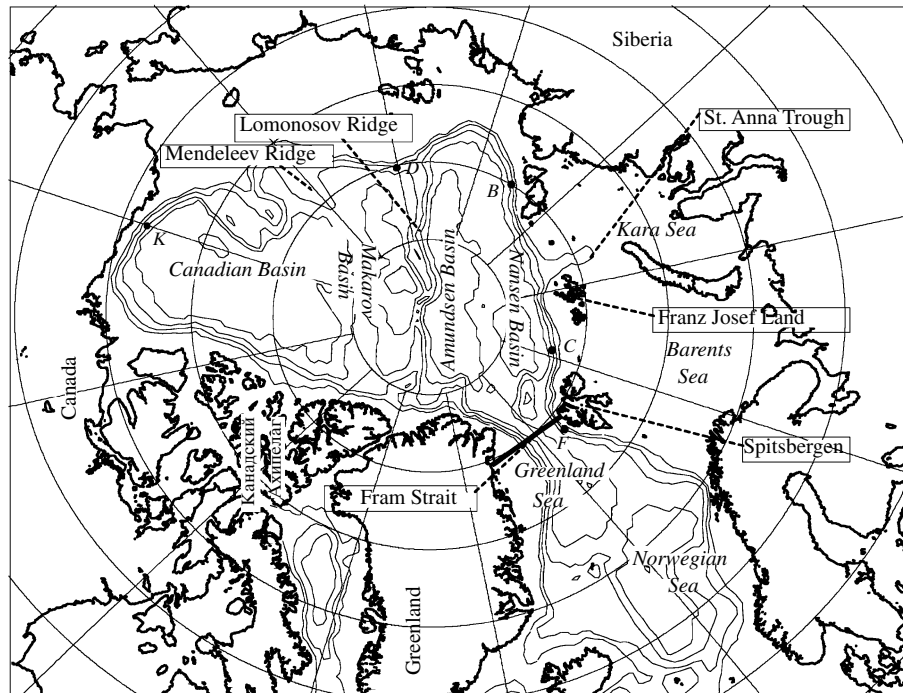


**Fig. 1.** Schematic of the Arctic Ocean bottom with the geographical names used in the text. The Lomonosov Ridge divided the Arctic Basin into the Eurasian and Amerasian subbasins. The Eurasian subbasin extends from the Lomonosov Ridge to the continental slope of Greenland, the Barents, Kara, and Laptev seas. The Amerasian subbasin is located from the Lomonosov Ridge to the continental slopes of the Canadian Archipelago, Alaska, Chukchi, and East Siberian seas.

In particular, this study addresses the effect of variations in the atmospheric circulation on the ice drift and circulation of the upper ocean layer, the change in the thermohaline structure of the Arctic Ocean waters, and the thermodynamics of the sea-ice cover. On the basis of the numerical experiment, we found that there are heating and cooling periods in the Atlantic water layer. The model reproduces the regimes of freshened water accumulation in the Canadian Basin in the period of anticyclonic gyre of surface waters and the regime of its flow through the Fram Strait and Canadian Archipelago channels in the period of cyclonic gyre. The model results indicate that the reconfiguration of the water circulation of surface and intermediate layers of the ocean caused by a phase shift of the North Atlantic circulation started in the mid-1970s.

## 1. FORMULATION OF THE NUMERICAL EXPERIMENT

The climate variability of the Arctic Ocean for the period from 1948 to 2007 has been investigated on the basis of the combined ocean–ice numerical model adapted to the region of the Arctic and northern Atlantic.

### 1.1. Structure of the Numerical Model

Oceanic processes are described using a numerical model of ocean dynamics that can be traced back to

the model of the world ocean circulation (developed in the Institute of Numerical Mathematics and Mathematical Geophysics of the Siberian Branch of the Russian Academy of Sciences) [17–19] adapted to the region of the Arctic and northern Atlantic and modified in the course of further investigations [20, 21]. The system of complete nonlinear equations of ocean thermohydrodynamics is written in curvilinear orthogonal coordinates with the traditional hydrostatic and Boussinesq approximations. At the ocean surface, the “rigid lid” approximation is used. The dynamic equations are solved by the method of separating barotropic and baroclinic modes; here, the barotropic mode is expressed as a solution of the stream-function equation. The problem is solved in time by a hybrid explicit–implicit scheme with the method of splitting into physical processes and spatial coordinates.

In the current version of the numerical model, the advection–diffusion equation of heat–salt transport is split into two equations. The first equation describes the process of transport, and the second describes the process of diffusion. For the diffusion equation, an implicit (in time) numerical scheme combined with the method of splitting into one-dimensional finite-difference equations is used. The equation describing transport by currents is approximated using the QUICKEST scheme [22]. The numerical algorithm of

the model is described in [20]. The results of applying the QUICKEST scheme can be found in [21].

The sea-ice model used by us (known as the elastic viscous–plastic model) is a modification of the standard viscous–plastic model of ice dynamics [23]. A detailed description of this model can be found in [24]. The thickness of snow cover and ice is calculated on the basis of a thermodynamic model [25] for each ice category. The horizontal advection of ice is treated with the help of an advection scheme of the semi-Lagrangian type [26].

### 1.2. Modeling Domain

The interaction between the Arctic Basin and northern Atlantic is simulated for the domain of the Arctic Ocean and northern Atlantic starting at 20° S. The grid resolution for the northern Atlantic is chosen to be 1°. On the circle of 65° N, the spherical grid adopted for the Atlantic is naturally coupled with another orthogonal grid of finer resolution. The second grid is constructed in the following way: a one-degree spherical grid of coordinate lines with ground-based poles is constructed on a small hemisphere with a diameter equal to the diameter of the circle of 65° N, and the resulting grid is projected onto the polar area limited by the circle of 65° N [27]. In this case, all coordinate lines of the second grid are orthogonal and turn at the latitude of 65° N to the corresponding coordinate lines of the spherical system. The maximum resolution is 35 km. On average, the nodes of the numerical grid of the Arctic Ocean area are located at a distance of about 50 km. The vertical distribution consists of 33 horizontal levels becoming denser near the surface, where the resolution is equal to 10 m. The modeling domain includes the most significant channels within the Canadian Archipelago. The minimum depth of the shelf zone is taken to be 50 m.

### 1.3. Initial Distribution

The initial distribution of fields of the combined system has an increased value especially for the deep-water section of the ocean. The thermohaline structure for deepwater layers has been generated over the course of hundreds of years. In this paper, a detailed study of this problem is not our task; however, we can accept its necessity in further studies. Therefore, the initial distributions, at least, must be as close to the real pattern as possible.

The initial distributions of temperature and salinity have been derived from a combination of the Levitus data and a series of oceanographic data collected by sensory investigations of the Arctic and the adjacent areas. The PHC climate data [28] have been obtained precisely in this way and constitute three-dimensional monthly distributions of temperature and salinity in the layer up to 1 km in depth, as well as seasonal (win-

ter and summer) and annual data for the total depth range. In particular, the winter distributions have been used as the initial distributions, because the start of numerical modeling was fixed to wintertime (January 1, 1948). In these data, the absolute temperature of water has been recalculated to derive the distribution of potential temperature, which is necessary for a correct account of vertical heat fluxes.

The ice field varies more dynamically than the thermohaline structure of the deep ocean; therefore, this field can be reconstructed in shorter periods with the help of the model itself. In line with the AOMIP recommendations, the preliminary numerical experiment was performed for the period from 1948 to 1954 to reconstruct the initial field of ice; in this case, the initial distribution is such that the ice thickness is equal to 2 m for areas where the surface temperature is lower than 0°C, while no ice can be found in other areas. The distributions of thickness and concentration that were obtained for all ice categories from this preliminary experiment are used for specifying the initial conditions of the main experiment performed for the period from 1948 to 2007.

The initial components of water and ice velocities are also obtained as a result of this preliminary experiment. The initial conditions for this preliminary experiment are assumed to be zero for the velocity components of both ice and water.

### 1.4. Conditions at the Bottom and Lateral Boundary of the Domain

The boundary conditions at the bottom and rigid lateral boundaries allow no heat or salt fluxes through these boundaries, and the current undergoes local bottom friction proportional to the square of bottom velocity. The southern boundary connecting the modeling domain with the southern Atlantic is liquid. The conditions at this boundary allow free advection outside the modeling domain if the velocity is directed toward this side. Otherwise, the values taken from PHC for the initial distributions of temperature and salinity serve as advection fluxes into the domain. We also specify the barotropic water flow corresponding to waters partially removed through this boundary. This flow is linearly distributed along the Atlantic width at the latitude of the southern boundary of the domain and compensates for the total river flow and inflow through the Bering Strait. The lateral conditions for liquid boundaries of ice are not presupposed, because the southern boundary is inaccessible and the Bering Strait is assumed to be close for ice drift.

The lateral boundaries for river freshwater inflow are given according to the existing data on the climatic mean seasonal variation of the runoff of 13 major rivers of the Arctic. The values of their flows are taken from the AOMIP database. The total runoff constitutes

8.6 km<sup>3</sup>/day. In addition, we take into account the runoff of 23 rivers in the northern and equatorial Atlantic (on the average, 29.7 km<sup>3</sup>/day) obtained from the River Discharge Database [29]. The specification of river flows is accompanied by the specification of freshwater inflow with the help of the following boundary condition on salinity:

$$-\mu_s \frac{dS}{dn} + (\mathbf{u} \cdot \mathbf{n})S = Q,$$

$$Q = -\frac{STr}{A},$$

where  $\mathbf{n}$  is the normal to the boundary through which the inflow occurs;  $u_n = (\mathbf{u} \cdot \mathbf{n})$  is the velocity in this direction;  $Tr$  is the magnitude of river flow;  $A$  is the area of the lateral boundary, which is equal to the product of  $\Delta l$  (the length of boundary section) by  $H$  (the depth of basin at this section); and  $\mu_s$  is the horizontal diffusion coefficient for salt. Similarly, we specify the water flow at the section of the Bering Strait, except that the salinity of water inflow is taken from the PHC data. Thus, we have

$$Q = \frac{(S_{\text{PHC}} - S)Tr}{A}.$$

### 1.5. Boundary Conditions at the Ocean Surface

The necessary conditions at the surface of the ocean–ice system are listed as follows:

(a) latent and visible heat fluxes, incoming solar and longwave radiation, and longwave surface radiation;

(b) wind friction;

(c) freshwater flow related to precipitation as snow and rain.

To calculate these characteristics, along with the inner parameters of the system (surface temperature, ice concentration, and ice categories), data on the parameters of the lower atmosphere and intensity of radiation balance terms are needed. The full list of necessary atmospheric data includes the velocity and direction of surface wind, potential and absolute temperature of the lower atmospheric layer; specific humidity; surface pressure and air density, total incoming solar and infrared radiation, and intensity of precipitation (snow and rain).

Because the precipitation in the initial data is not directly divided into fractions, it is additionally assumed to be snow if the surface temperature is negative and rain if the surface temperature is positive.

In the numerical experiments, the lower-atmosphere characteristics obtained from several sources have been used. One of the most complete atmospheric databases is the NCEP/NCAR Reanalysis data [10]. Many deficiencies of this database have been

eliminated in the subsequent modification described in [16]. Abbreviated as CIAF, this database is available free on the Internet and has the same resolution and periodicity as NCEP/NCAR reanalysis data.

## 2. SPECIFIC FEATURES OF ATMOSPHERIC CIRCULATION IN THE NORTHERN ATLANTIC

Before we analyze the numerical modeling results, let us note the most important features of the atmospheric circulation, which is the main driving force in the experiments. One of the main modes of atmospheric variability in the Northern Hemisphere is the North Atlantic Oscillation (NAO) [30]. The latter reflects the oscillation of atmospheric masses between the north and south of the North Atlantic, with centers near Iceland (Icelandic Low) and Azores (Azores High). The state of NAO is estimated using the index defined as the difference of pressure anomalies at the sea level between the Azores High and Icelandic Low. Although the interplay between atmospheric centers of action manifests itself in the course of the whole year, the amplitude of oscillations is maximal in the winter season, when the atmosphere is most active dynamically. Therefore, the index values calculated for the winter season from December to March are normally considered.

Starting with the classical study by V.V. Shuleikin [31], self-oscillation functioning regimes of the North Atlantic–Arctic Ocean system have repeatedly been put forward by researchers. In [32] it was supposed that there are Arctic climatic cycles of some 15–20 years related to the NAO phases.

In the period of the negative NAO phase, the intensity of the Azores High and Icelandic Low is below the average values. This leads to a decreased intensity of westerly winds, which shift their direction to the Mediterranean Sea. In the Arctic, a high pressure is dominant and the cold regime of the anticyclonic gyre is initiated. The river runoff is decreased, which leads to a decreased water salinity in the surface layer. The ocean accumulates fresh water by increasing the volume of freshened water in the Beaufort Sea and increasing the thickness and length of ice through an increased rate of ice growth.

The positive NAO phase corresponds to the increased intensity of baric centers and their northward or northwestward shift. The gradient increase is accompanied by intensified winds carrying warm and humid air from the Atlantic Ocean into northern Europe. In the Arctic, a low atmospheric pressure (cyclonic gyre regime) is dominant, which corresponds to the warming period. The warming leads to strong ice melting; however, the cyclonic gyre regime is unfavorable for freshwater conservation in the Arctic Basin. A large amount of freshwater goes into the

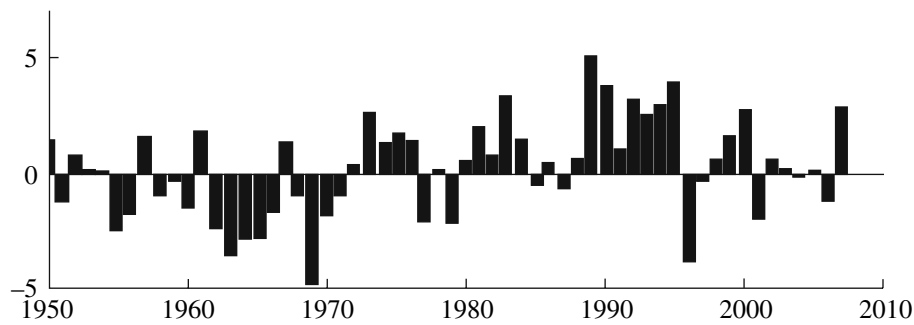


Fig. 2. NAO index in the period from 1950 to 2007 from the data given at <http://www.cpc.ncep.noaa.gov>.

northern Atlantic through the Fram Strait and Canadian Archipelago channels, leading to salinity anomalies in northern seas and decreased deep convection and reduced deepwater generation.

A study of the effect of two NAO phases on the state of the Arctic Ocean on the basis of the existing observational databases is presented in [33]. The data on the NAO index, for which a long-term time series has been constructed [34] (Fig. 2), are freely accessible on the official site of the National Oceanic and Atmospheric Administration (NOAA) at <http://www.cpc.ncep.noaa.gov>. An extended period of the negative NAO phase was recorded from 1960 to the mid-1970s. Starting in the mid-1970s, the turn to the positive phase was accompanied by a stable trend of the index to increase. In the winter of 1989, an absolute maximum of the NAO index was reached; then, its value started to decrease. In the period between 1980 and 2007, negative values of the NAO index have been recorded only in individual years.

In the subsequent sections, we describe the variability of the ocean–ice climate system of the Arctic Ocean obtained by numerical modeling as a response to variations in the atmospheric circulation over the second half of the twentieth century.

### 3. TWO REGIMES OF ICE DRIFT AND SURFACE CIRCULATION OF WATERS IN THE ARCTIC OCEAN

#### 3.1. Information Derived from Observational Data and Scientific Hypotheses

Lomonosov's hypothesis on the existence of a general east-to-west ice drift in the Arctic Ocean was confirmed by drifts of the following vessels: *Jeanette* (1879–1881), *Fram* (1893–1896), and *Sedov* (1937–1940). Monograph [35] presents researchers' different views on the nature of the surface current and ice drift in the Arctic Basin that existed in the middle of the twentieth century. According to one view, the surface current and ice drift in the central sector of the Arctic Basin were regarded as a compensatory current with respect to the incoming Atlantic waters. Here, the ice

and surface waters of the Arctic Basin were assumed to be transported to the Fram Strait on the shortest route. The proponents of another view assumed that the ice drift and the surface current are governed mainly by the atmospheric circulation over the Arctic Ocean and can generate an anticyclonic gyre. The observational data of the 1949, 1950, and 1956 high-latitude aerial expeditions, the 1951 and 1952 American expeditions, and the drift of “Severny Polys-2” station that started in 1951 confirmed the existence of the anticyclonic gyre of surface waters. All ice floes that later hosted drifting stations were characterized by a general drift toward the Fram Strait. Based on the processing of data obtained by these expeditions, A. F. Treshnikov [36] constructed the first map of dynamical heights, indicating a wide belt of the transpolar drift from the Bering Strait toward the Fram Strait, the Eastern anticyclonic gyre in the American subbasin, and a cyclonic pattern of the circulation south of the Transpolar Current.

The position and size of the Trans-Arctic Current and the Eastern anticyclonic gyre are subjected to seasonal and interannual oscillations caused mainly by a change in the field of atmospheric pressure. By comparing the distribution of atmospheric pressure with observational data on currents, Z.M. Gudkovich [37] characterizes two types of surface circulation waters and ice drift. The first type of circulation corresponds to the period of a strong polar anticyclone. This period is characterized by an extensive Eastern anticyclonic gyre, a shift of the Transpolar Current to the Eurasian shores, and an ice transport from the Siberian seas into the Greenland Sea. The second type of circulation emerges in the period of dissipation of the polar anticyclone, shifting it to Canada and significantly developing the Siberian atmospheric maximum with a turn to the East Siberian seas. In this case, the axis of the Trans-Arctic Current is shifted to North America. In [38], it was suggested that the coefficient of correlation between atmospheric circulation and the 200-m layer of the Arctic Ocean is 80%.

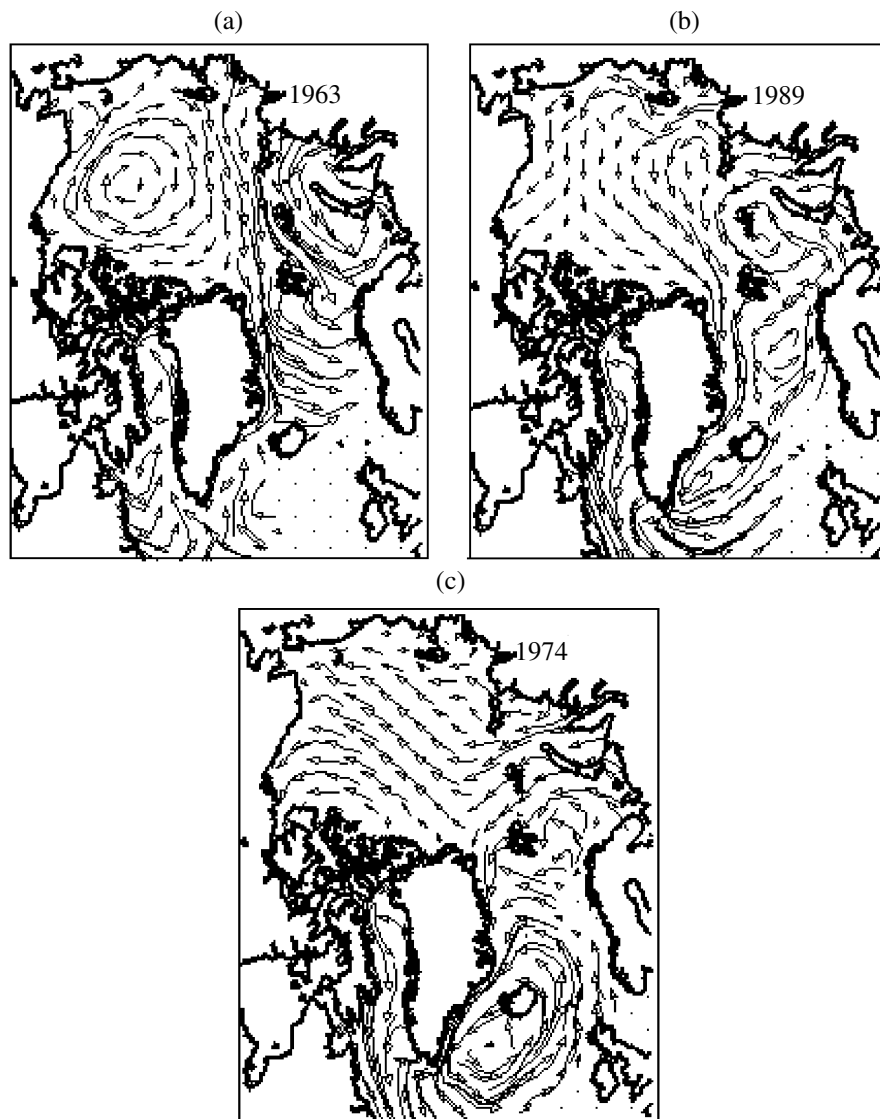


**Fig. 3.** Winter ice-drift distribution according to numerical calculations. The fields characterize different periods: (a) the 1963 distribution characterizes an anticyclonic system of ice drift, (b) the 1989 distribution is an example of cyclonic gyre, and (c) the 1974 distribution is a transition form between the two main circulation types.

### 3.2. Results of Numerical Modeling

The pattern of ice drift obtained by numerical modeling largely reflects the specific features of atmospheric circulation, among which seasonal oscillations prevail. In addition, the results clearly indicate two ice-drift regimes: cyclonic and anticyclonic. The period of anticyclonic gyre is characterized by a clearly expressed anticyclonic pattern covering most of the Arctic Basin (Fig. 3a). In the model, this state corresponds to the periods of the 1960s and from 1975 to 1988, excluding a few years.

In the period of a cyclonic gyre, the flow coming from northern seas is intensified, the anticyclonic wind becomes weaker, and the trajectory of the transpolar drift is shifted to the Canadian coast. Figure 3 shows the pattern

of ice drift for the period of a cyclonic gyre. In model calculations, the cyclonic gyre corresponds to the period between 1989 and 1994. Evidently, there are intermediate states between the corresponding periods; for example, the 1974 distribution (see Fig. 3c). The calculated periods of a clearly expressed type of circulation are shown in Table 1. Two types of circulation in the Arctic Basin were reconstructed on the basis of a numerical barotropic model described in [39]. The distribution obtained by us is partially consistent with these results; however, there are also some discrepancies in determining specific periods, which are caused, most likely, by the existing data on ocean surface sources. The experimental results are generally consistent with observational data on ice drift (see

<http://iabp.apl.washington.edu> for the description of these data).

An analysis of the calculation results indicates that the ice drift is related to the NAO index. Positive values of this index normally correspond to the cyclonic vorticity of ice drift. No strong relationship between its negative values and the anticyclonic drift vorticity can be traced, and it can be inferred from here that this vorticity is more reasonable for the Arctic Basin and emerges whenever no anomalously high values of the NAO index are found. The coefficient of the correlation between the NAO index and the ice circulation around Spitsbergen and Franz Joseph Land is 0.55. The same coefficient is equal to 0.40 for the circulation around the North Pole and 0.34 for the circulation around the Canadian Basin.

#### 4. TWO STATES IN THE SALINITY DISTRIBUTION OF THE ARCTIC OCEAN SURFACE LAYER

The small area of the Arctic Ocean acquires a huge amount of freshwater by river runoff. This freshwater is important for the formation and conservation of the special structure of the Arctic halocline and thermohaline circulation. The water surface layer is also freshened both by snow and sea-ice melting and because there is more precipitation than evaporation. The freshwater flow is balanced by the water runoff through the Fram Strait and Canadian Archipelago; however, the freshening area is characterized by considerable spatial and temporal variations caused by seasonal and interannual oscillations of the climate system. The main hypothesis proposed in [40] assumes the following.

(a) In the period of an active anticyclonic gyre of the atmosphere in the Arctic region, the increased anticyclonic gyre of surface waters leads to the concentration of a significant amount of freshwater in the Beaufort Sea from different sources.

(b) In the period of the cyclonic regime characterized by low atmospheric pressure, the Arctic involves a growing cyclonic surface-water circulation assisting the freshwater outflow through the Fram Strait and Canadian Archipelago channels rather than supporting its concentration in the Beaufort Sea.

An analysis of the numerical experiment for the period from 1948 to 2007 has indicated that there are two regimes of the distribution of salinity in the ocean surface layer. The numerical experiment reveals that advection is one of the most important processes responsible for the variability of salinity in the Arctic Ocean. In the period of the well-developed anticyclone and 1960–1980 negative NAO phase, there has been a freshwater accumulation in the center of the Beaufort circulation in the Canadian Basin. Figure 4 shows the averaged (over the upper 100 m-layer)

**Table 1.** Calculated periods of the two types of ice-drift circulation

Type of circulation	Calculated lifetime
Anticyclonic	1960, 1961, 1963, 1965, 1966, 1969, 1970–1973, 1977–1980, 1982–1983, 1985–1986, 1988, 1992, 1994, 1996, 1998, 2001
Cyclonic	1967, 1968, 1981, 1984, 1989, 1993, 1995, 1997, 1999, 2000, 2002, 2003

salinity field for a 20-year period; mostly, this corresponds to the active anticyclonic period in the Arctic. Because of the anticyclonic gyre initiated in the upper 100 m-layer in the Amerasian Basin by 1970, a closed area with a fresher water mass of a salinity value less than 31.5‰ appeared. One can clearly see the trajectory of the signal propagation from the Siberian rivers with the involvement of the circulation. It should be noted that, in 1960, the salinity distribution in the Amerasian Basin had a quite different form. By 1980, the salinity kept its structure and the least freshwater area, with a salinity of less than 31‰, was slightly extended.

The change of the surface water circulation to the cyclonic one in the late 1980s led to changes in the salinity fields (Fig. 4). In contrast to the previous pattern, the signal propagates from the Siberian rivers to the east in accordance with the cyclonic gyre. The western section of the Arctic Basin is filled with water intensely flowing from the Fram Strait and Barents Sea. With time, the tongue of more saline water propagates along the area corresponding to the position of the continental slope. The freshwater area is shifted to the Canadian coast. The cyclonic gyre does not support the accumulation regime, and the freshwater flows out gradually through the Fram Strait and Canadian Archipelago channels.

Thus, the numerical experiment confirms the hypothesis on freshwater accumulation in the Canadian Basin of the Arctic in the period characterized by the anticyclonic motion of surface waters and on the discharge of the reserve of accumulated freshwater in the period of a cyclonic gyre. It should also be noted that, in this experiment, the main mechanism responsible for this process is advection, because the interannual variability of the river flows was not taken into account. This conclusion is consistent with the results obtained in [41].

#### 5. VARIATIONS IN THE ATLANTIC WATER LAYER OF THE ARCTIC BASIN

##### 5.1. Observational Data

Warm intermediate waters of the Atlantic origin constitute one of the key features of the Arctic Ocean

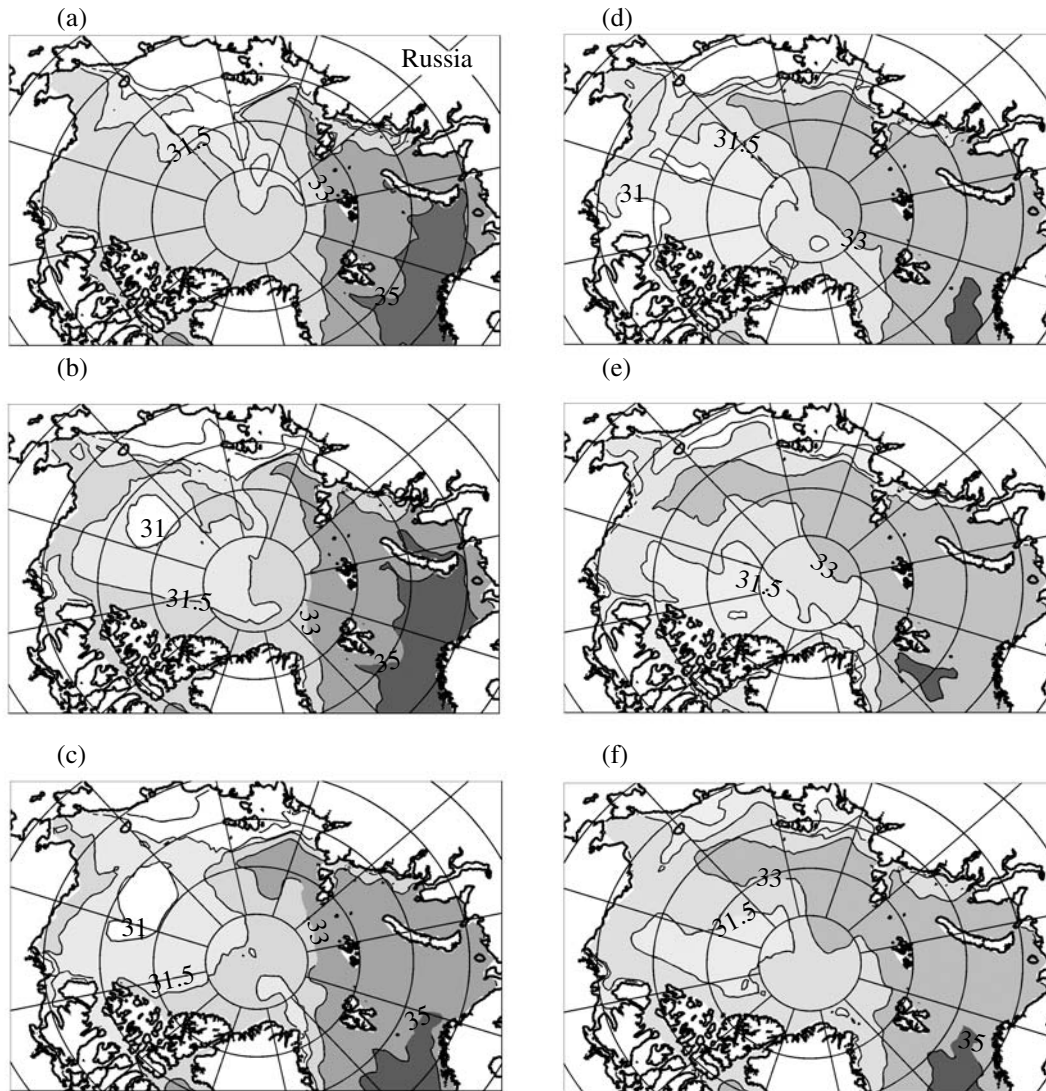


**Fig. 4.** Averaged salinity (in ‰) in the layer between 0 and 100 m. Freshwater accumulation in the Canadian Basin in the period of anticyclonic surface-water circulation (from 1960 to the late 1980s). Freshwater flow through the Fram Strait and Canadian Archipelago straits in the period of cyclonic gyre (1989–2000): (a) 1960, (b) 1970, (c) 1980, (d) 1990, (e) 1995, and (f) 2000.

climate. Two branches of Atlantic waters flow into the Arctic Basin through the Norwegian Sea. The eastern branch passes through the Barents Sea, where the Atlantic water loses most of its heat due to a strong exchange through the sea surface. The second branch of Atlantic waters (the western Spitsbergen Current) penetrates into the Arctic Basin through the Fram Strait. Mixing with the cold Arctic water, this current goes down to the level of intermediate waters and then moves eastward along the continental slope. This branch of Atlantic waters is the main source of heat in the Arctic Basin.

The sharp increase in temperature in the layer of Atlantic water in 1990 was the first indicator of climate changes occurring in the Arctic. A temperature

exceeding climatic values was recorded in 1990 in the Nansen Basin [1]. By 1993, an increase in temperature in the Amundsen [4] and Makarov [2] basins was observed.

The variability of properties of Arctic waters was studied [42] using the open database of 1948–1993 measurements under the Joint Russian–American Commission program on economic and technological collaboration (Environmental Working Group, 1997). An analysis of the existing data allowed the authors of that study to reveal several cold and warm periods in the layer of Atlantic waters (Table 2). The warm period is fixed to the mid-to-late 1950s, from 1963 to 1969, and from the 1990s to present. The 1950s and 1990s warming events in these data manifests itself as

**Table 2.** State of the Arctic Basin according to the 1977 data of the Environmental Working Group

Period	State	Hypothesis
From 1955 to the late 1950s	Warming	Flow of warm waters through the Fram Strait and heat-anomaly transfer by the boundary current
1963–1969	Warming	Reduction of the heat loss in the Atlantic layer because of surface-water freshening and intensified vertical stratification
From 1974 to the late 1980s	Cooling	Flow of anomalously cold waters out of the Laptev and Kara seas
1989–1993	Warming	Flow of warm waters through the Fram Strait and heat-anomaly transfer by the boundary current

a heat signal propagating in the flow of the boundary current through the Fram Strait; however, the warming in the 1950s was not as significant as the warming in the 1990s. By the early 1960s, the temperature in the Eurasian Basin substantially decreased. The next wave of warming in observational data is recorded for the mid-to-late 1960s. Here, there are no indications of heat-signal propagation along the continental slope like in the 1950s and 1990s. In contrast, the cold state in 1960 and 1961 in the Eurasian and Canadian basins simultaneously changed to intense warming by 1963, which continued up to 1969. In [42], the authors proposed to explain the warming by the reduction of heat losses in the core of Atlantic waters because of the increased vertical stratification of waters through the surface-layer freshening. Indeed, the existing data may be indicative of a reduced salinity in the ocean surface layer in this period. However, because of a lack in detail for the 1960s salinity data, this explanation was proposed as a hypothesis.

The cold period was pointed out for an area located east of 37° E between 1974 and the late 1980s. Supposedly, this was caused by the intense cooling of shelf waters flowing into the Arctic Basin from the Laptev and Kara seas.

### 5.2. Results of Numerical Modeling

An analysis of the temperature distribution obtained from numerical experiments made it possible to reveal the response of the model ocean to the changing atmospheric effect. Figure 5 shows the temporal variation of the vertical distribution of temperature at given points along the boundary current of the Atlantic water motion. The warming process of the 1960s (1963–1969 in Table 2) known from observational data is present in the calculation results mainly for the Eurasian Basin (points B and D; see the allocation of points in Fig. 1). It can be seen from Figure 5 that there is no heat signal in the Fram Strait (point F) during this period. On the average, an increase of 1.08°C in the water temperature in the layer from 100 to 200 m in an area between Severnaya Zemlya and the Lomonosov Ridge was found for this period. In

this case, in line with the hypothesis of [42], the surface-layer salinity in the Eurasian Basin in the numerical experiment for 1960–1961 was really decreased on the average by 0.52‰, which contributed to the enhanced stratification and reduced heat loss in the flow of Atlantic waters.

The next period in the numerical calculations determines the cooling period for the regions east of the Severnaya Zemlya, which is consistent with the results of [42], where it was indicated that the cold Atlantic layer could be found by 1974 in the majority of measurement data. Supposedly, this cooling period is related to the cold anomaly in the Laptev and Kara seas. The results of our calculations indicate that there was an area of decreased temperature near the St. Anna Trough in the early 1970s. Let us note that the direction of motion in the field of ice drift for 1974 (Fig. 3) is really consistent with the hypothesis on the water outflow from the space of these seas. The further motion of waters led to the evolution of convective mixing and cooling of the Atlantic layer. In Fig. 5 this process is reflected by embedded isotherms. The period of cooling of the Atlantic layer is from 1970 to 1978 in the distribution for point B located near Severnaya Zemlya and for point D located near the Novosibirsk Islands in the beginning area of the Lomonosov Ridge. In the Canadian Basin (point K), the cooling extends up to the mid-1980s.

The new warming wave appeared in the late 1980s, propagated in the cyclonic direction along the continental slope, and reached the Canadian Basin in the late 1990s (Fig. 5, point K). An analysis of observational data and model calculations [43] indicates that the propagation of heat anomaly in the early 1990s was caused by an increased positive NAO index, which led to an increased transport of the western Spitsbergen Current. In addition to the data of changed temperature at the given points, Fig. 6 shows the field of ocean temperature at a depth of 200 m for certain periods. The horizontal fields characterize the processes described above: the mid-1970s cooling of the layer of Atlantic waters and the heat-signal propagation along the continental slope in the 1990s.

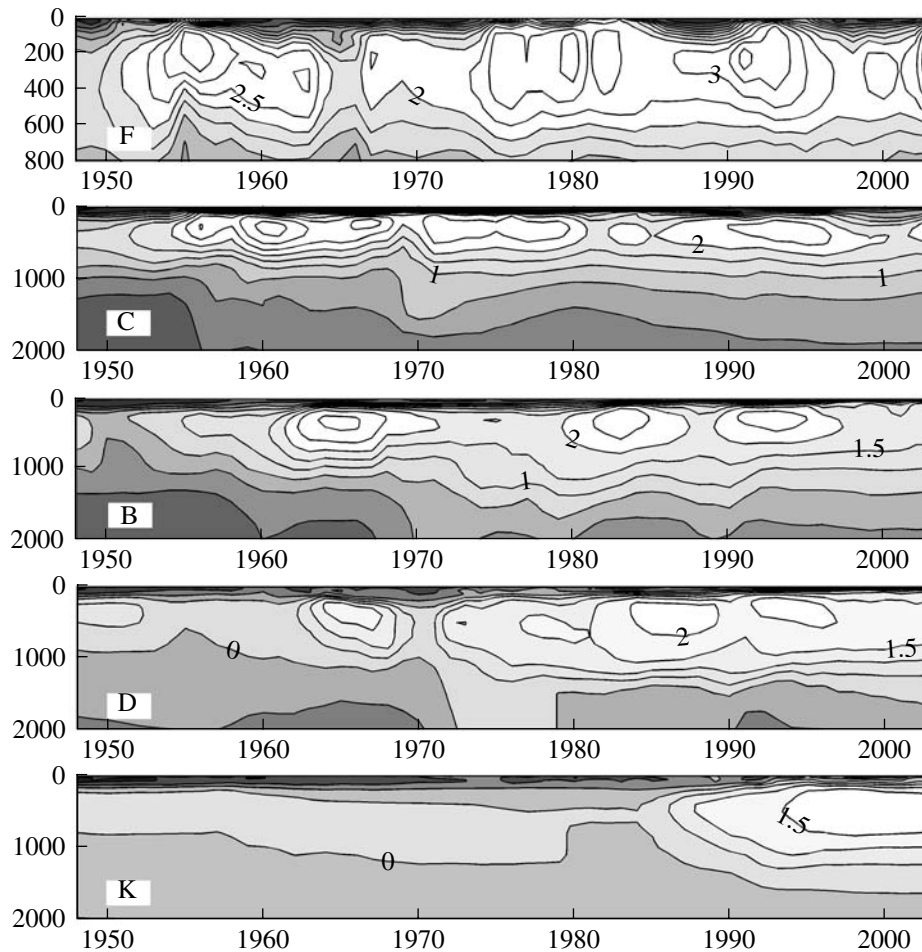


**Fig. 5.** Temporal evolution of temperature at the given points F, C, B, D, and K along the course of the boundary current transporting Atlantic waters. The allocation of the points is shown in Fig. 1.

## 6. EASTWARD SHIFT OF THE BOUNDARY BETWEEN ATLANTIC AND PACIFIC WATERS

### 6.1. Observational Data

The biogenic-rich Pacific waters play an important role in the biogeochemical regime of the Arctic Ocean. Passing the Bering Sea and the Chukchi Sea shelf, these waters move down along the shelf slope and propagate further as a relatively warm current. In the Amerasian Basin, the Pacific waters generate upper thermohaline waters occupying the intermediate layer between the relatively fresh Arctic surface waters (0–100 m) and the warm and saline waters of the North Atlantic origin, thus being a kind of inter-layer opposing the motion of Atlantic waters toward the ice surface. In spite of the fact that the Pacific waters have been substantially modified in passing the Bering and Chukchi seas, their chemical characteristics are conserved, thus allowing one to identify their origin. In the past, the existence of these waters was clearly traced up to the Amerasian Basin boundary (the Lomonosov Ridge) [44, 45].

On the basis of the observed changes in the chemical composition of waters in 1991, the location of the water-partitioning front has been assumed to be variable [46]. According to the 1993 measurement data for the southern part of the Canadian Basin, there was an eastward shift of the boundary between the Atlantic and Pacific water masses [47]. The initial position of this boundary near the Lomonosov Ridge was shifted into the Mendeleev Ridge. In the EWG measurement data [42] for the period 1948–1993, the presence of the Pacific water mass was determined by a maximum in the vertical distribution of  $\text{SiO}_3$  at a depth of between 50 and 150 m. An analysis of the database has demonstrated that the sharp disappearance of features of the Pacific water mass in the Makarov Trough and northern part of the Nansen Basin occurred between 1984 and 1985.

### 6.2. Results of Numerical Modeling

According to numerical results, the flow field of ocean subsurface and intermediate layers is character-

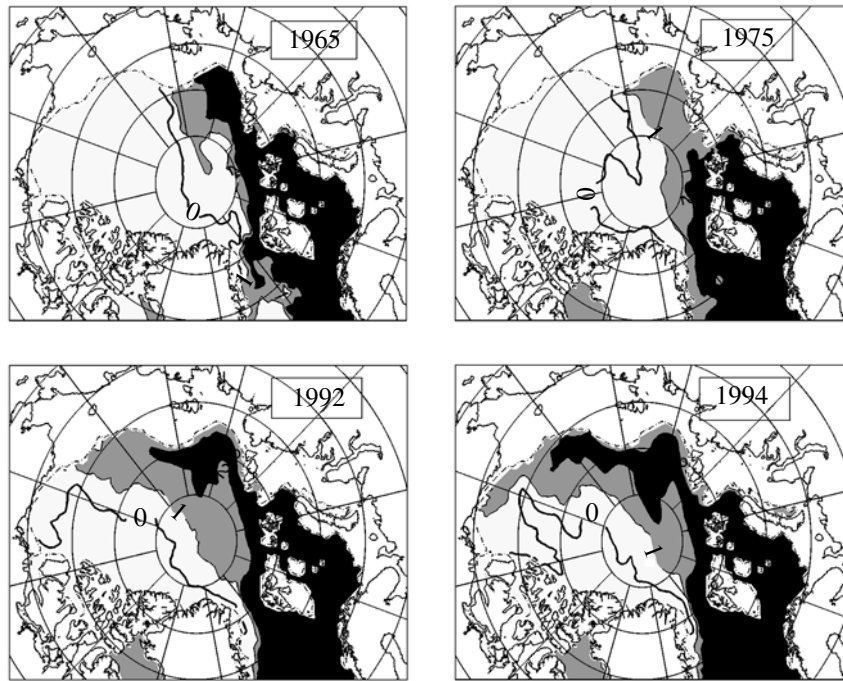


**Fig. 6.** Variation in the distribution of temperature at a depth of 200 m calculated by the combined ocean–ice model. The periods of Arctic cooling in the mid-1970s and heat-anomaly propagation in the 1990s are demonstrated. Here, the isotherms 0, 1, and 2°C are shown.

ized by substantial changes during the period under consideration. The flow field averaged over the layer from 50 to 150 m (see Fig. 7) describes the interaction between the two major (Pacific and Atlantic) water masses entering the Basin. It is this layer that is assumed to involve the propagating Pacific waters. The water circulation initiated by the late 1960s is substantially different at these depths for the Amerasian and Eurasian basins. The Eurasian section is occupied by a flow of Atlantic waters propagating through the Barents Sea and Fram Strait in the cyclonic direction along the continental slope. The vast Amerasian Basin is an area with an anticyclonic gyre that also includes the Pacific waters. The area of the Lomonosov Ridge is the boundary between the Atlantic and Pacific waters over this period.

The system of water circulation started to rearrange itself in the mid-1970s, when the model flow field was observed to involve a penetrating current of Atlantic waters east of the Lomonosov Ridge, which was earlier unknown at these depths. A comparison with the NAO index distribution (Fig. 2) indicates that it is the mid-1970s that marked the transition period initiating the positive NAO phase and enhancing the cyclonic motion in the Arctic Ocean. Throughout the subsequent twenty years, a gradually changing pattern of circulation and the establishment of cyclonic water motion in the Canadian Basin by 1990 were observed. A detailed analysis of the water circulation pattern

between 1980 and 1985 demonstrated that, according to the numerical results, the central Arctic was dominated by Pacific waters at a depth of 100 m until 1985. After 1985, the flow transporting the Pacific waters was displaced by the Atlantic waters. In view of the fact that the model does not take into account the variability of interannual flow through the Bering Sea, these processes cannot be caused by a reduced transport of Pacific waters. This shift is not a simple reflection of the changing situation in the wind field at the ocean surface, which is more typical of ice drift. The experimental results show that the process of rearranging the circulation of subsurface waters is also conditioned by the internal dynamics of the basin, which is determined by the water flows entering through the straits (in this case, by the flow of Atlantic waters).

Since the mid-1980s, the boundary between the two water masses lies near the Mendeleev Ridge. The process described above is confirmed by the temporal evolution of temperature at point K (see Fig. 5), where a heat signal was found in the mid-1980s, indicating that the Atlantic waters flowed into the Canadian Basin.

The Pacific water circulation scheme proposed in [48] and the explanation of the occurring boundary shift are absolutely opposite to Fig. 7. According to the hypothesis proposed in [48], the circulation of the Pacific water mass has always occurred in the cyclonic

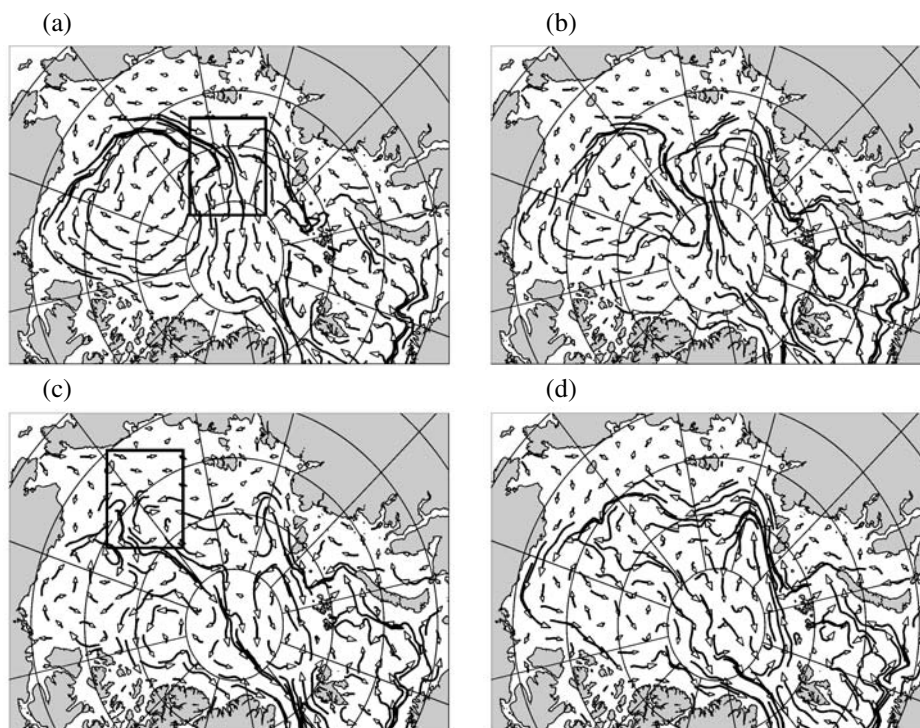


**Fig. 7.** Calculated shift between the Atlantic and Pacific waters. The flow field averaged over the layer 50–150 m: (a) 1970, (b) 1980, (c) 1985, and (d) 1992. The rectangle marks the area of the boundary between water masses.

direction only. However, we note that our results are consistent with the modeling results of [49]. In addition, the plots of vertical distribution shown in [42] demonstrate that the maximum value of  $\text{SiO}_3$  (the main distinctive feature of the Pacific water mass) in the Makarov Trough in the period preceding 1985 is higher than that in the central part of the Arctic Basin, which testifies that the Pacific waters in those years might propagate in the cyclonic direction.

## 7. REDUCTION OF ICE AREA IN THE ARCTIC OCEAN

### 7.1. Observational Data

According to observational data, the Arctic is characterized by growing (in the recent decades) warming accompanied by reduced area and thickness of sea ice in the Arctic Ocean. In [6], one can find a brief review of scientific papers reporting on the process of ice-cover reduction in different areas of the Arctic. According to data of the National Snow and Ice Data Center, the linear trend in the reduction of sea-ice area from 1979 to 2005 was more than 8% per decade. According to recent data, a substantial reduction of the minimum ice-cover length occurred in 2007. The absolute minimum of 5.7 millions  $\text{km}^2$  for September, 2005, decreased further to 4.28 millions  $\text{km}^2$  (Fig. 8). This event is said to be caused by the set of atmospheric conditions initiated in 2007 in the central Arc-

tic and Siberian shelf area, contributing to a faster ice melting in the central Arctic and ice driving off the Siberian shelf (press release of the National Snow and Ice Data Center, <http://nsidc.org/news/press>).

### 7.2. Results of Numerical Modeling

The periods of atmospheric circulation repeatedly considered in this study assisted in reconstructing an adequate pattern of the ice situation in the model experiments. According to the results of numerical experiments, the first and largest ice was formed in the central part of the Canadian Basin. By early 1980, the ice thickness in the center reached 6.6 m. This is an overestimated value, which points to the deficiency of the numerical model. A finer ice thickness could be found in the Laptev (about 3 m), Kara (about 2 m), and Barents (1–0.5 m) seas. The transition to the cyclonic type of circulation in the late 1980s and the subsequent warming led to the fact that the maximum values of ice thickness were shifted to the Canadian coast, the ice was driven off through the Fram Strait, and the thickness of Arctic ice gradually decreased. The dynamics of ice growth and melt calculated in the numerical experiment is shown in Fig. 9, which presents the temporal evolution of the sea-ice area for winter and summer distributions in a reference period. The trend to ice-cover reduction in summer can be

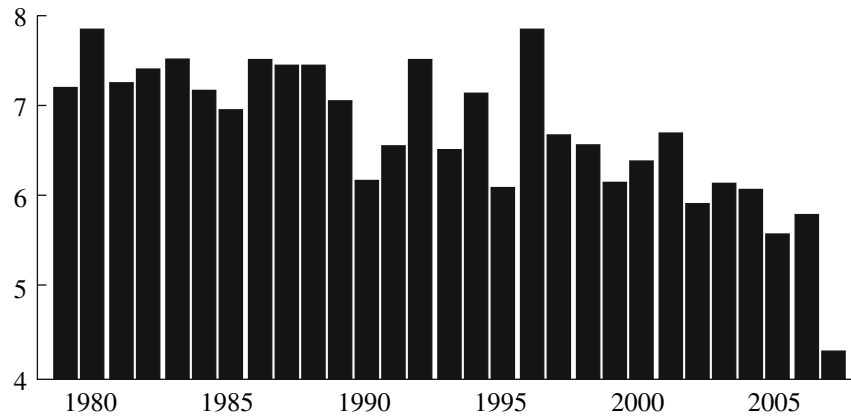


**Fig. 8.** Temporal variation of the ice-cover length (in  $10^6 \text{ km}^2$ ) for September based on data of the National Snow and Ice Data Center (<http://nsidc.org/news/press>). The linear trend of the length reduction has been estimated to be more than 8% per decade for the period 1979–2005.

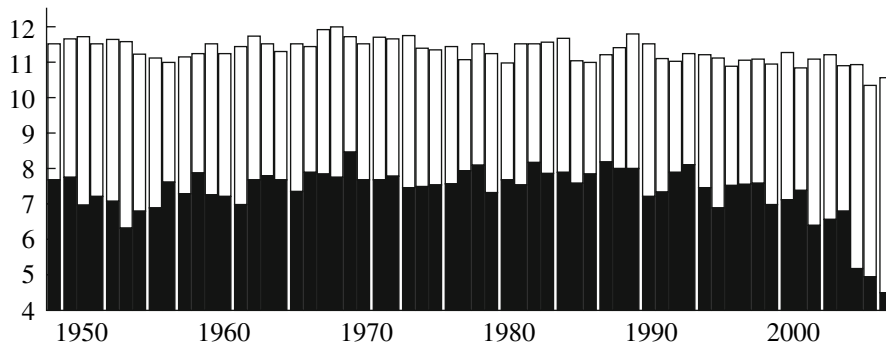


**Fig. 9.** Temporal variation of the ice-cover area (in  $10^6 \text{ km}^2$ ) calculated in the numerical experiment. The light rectangles correspond to maximum values, and the dark rectangles correspond to minimum values.

clearly seen in recent years. The absolute minimum was reached for 2007.

### 8. CONCLUSIONS

The numerical experiment, performed on the basis of the combined ocean–ice model for the period 1948–2007 by using NCEP/NCAR and CIAF atmospheric data, allowed us to reproduce the climate changes in the Arctic Ocean caused by variations in the atmospheric circulation.

The results of numerical experiments are the following.

(1) The two main regimes of the ice-cover circulation in the Arctic Basin are reproduced: cyclonic and anticyclonic regimes conditioned by variations in the atmospheric circulation.

(2) According to experimental data, the beginning of changes in the water circulation of the Arctic Ocean corresponds to the mid-1970s, which coincided with the first positive signal of the initiated positive NAO phase.

(3) During the negative NAO phase in the period 1960–1980, in line with the anticyclonic water circulation, the Canadian Basin is characterized by the formation of a wide low-salinity lens corresponding to the accumulation of freshwater flowing from rivers. In the subsequent period of the positive NAO phase, which facilitates the evolution of cyclonic motion of waters, the accumulated freshwater reserve flows into the northern Atlantic through the Canadian Archipelago channels and the Fram Strait.

(4) According to the numerical calculations, because of the initiation of the positive NAO phase, the flow of Atlantic waters into the Arctic Basin is enhanced, the boundary between the Atlantic and Pacific waters is shifted eastward, the water circulation in the Canadian Basin turns from anticyclonic to cyclonic, the temperature of the ocean intermediate layer grows, and the ice cover is reduced.

### ACKNOWLEDGMENTS

This study was supported by the Russian Foundation for Basic Research, project nos. 08-05-00457 and

08-05-00708, by the Division of Mathematical Sciences of the Russian Academy of Sciences, project no. 1.3.9, and by Rosobrazovanie, project no. 456 (05.06.2007) "Innovational Educational Programs and Technologies on the Basis of Partnership between Classical Universities, Science, Business, and State."

## REFERENCES

1. D. Quadfasel, "Warming in the Arctic," *Science* **350**, 385 (1991).
2. E. Carmack, R. Macdonald, R. Perkin, et al., "Evidence for Warming of Atlantic Water in the Southern Canadian Basin of the Arctic Ocean: Evidence from the Larsen-93 Expedition," *Geophys. Rev. Lett.* **22**, 1061–1065 (1995).
3. G. V. Alekseev, L. V. Bulatov, V. F. Zakharov, and V. V. Ivanov, "Thermal Expansion of Atlantic Waters in the Arctic Basin," *Meteorol. Gidrol.*, No. 7, 69–78 (1998).
4. J. Morison, M. Steele, and R. Andersen, "Hydrography of the Upper Arctic Ocean Measured from the Nuclear Submarine U.S.S. Pargo," *Deep-Sea Res.* **45**, 15–38 (1998).
5. R. W. Lindsay and J. Zhang, "The Thinning of Arctic Sea Ice, 1988–2003: Have We Passed a Tipping Point?," *J. Clim.* **18**, 4879–4894 (2005).
6. D. A. Rothrock, Y. Yu, and G. A. Maykut, "Thinning of the Arctic Sea-Ice Cover," *Geophys. Rev. Lett.* **26**, 3469–3472 (1999).
7. I. V. Polyakov, A. Beszczynska, E. C. Carmack, et al., "One More Step toward a Warmer Arctic," *Geophys. Rev. Lett.* **32**, doi: 10.1029/2005GL023740, L17605 (2005).
8. V. P. Dymnikov, V. N. Lykosov, and E. M. Volodin, "Problems of Modeling Climate and Climate Change," *Izv. Akad. Nauk, Fiz. Atm. Okeana* **42**, 618–636 (2006) [*Izv., Atmos. Ocean. Phys.* **42**, 568–585 (2006)].
9. S. Manabe and R. J. Stouffer, "Multiple-Century Response of a Coupled Ocean–Atmosphere Model to an Increase of Atmospheric Carbon Dioxide," *J. Clim.*, No. 7, 5–23 (1994).
10. E. Kalnay, M. Kanamitsu, R. Kistler, et al., "The NCEP/NCAR 40-Year Reanalysis Project," *Bull. Am. Meteorol. Soc.*, No. 77, 437–471 (1996).
11. V. A. Ryabchenko, G. V. Alekseev, I. A. Neelov, and A. Yu. Dvornikov, "Simulation of Climate Changes in the Arctic Basin with an Ocean–Ice Circulation Model without Reference to Climatic Salinity on the Ocean Surface," *Tr. AANII, Climate Change and Ocean–Atmosphere Interaction in Polar Regions* **446**, 60–82 (2003).
12. N. G. Yakovlev, "Coupled Model of Ocean General Circulation and Sea Ice Evolution in the Arctic Ocean," *Izv. Akad. Nauk, Fiz. Atm. Okeana* **39**, 394–409 (2003) [*Izv., Atmos. Ocean. Phys.* **39**, 355–368 (2003)].
13. S. N. Moshonkin, N. A. Dianskii, D. A. Eidinov, and A. V. Bagno, "Simulation of the Coupled Circulation of the North Atlantic and Arctic Ocean," *Okeanologiya* **44**, 811–825 (2004).
14. G. Holloway, F. Dupont, E. Golubeva, et al., "Water Properties and Circulation in Arctic Ocean Models," *J. Geophys. Res.* **112**, doi: 10.1029/2006JC003642, C04S03 (2007).
15. O. M. Johannessen, L. Bengtsson, M. W. Miles, et al., "Arctic Climate Change: Observed and Modelled Temperature and Sea Ice Variability," *Tellus A* **56**, C. 328–341 (2004).
16. W. G. Large and S. G. Yeager, "Diurnal to Decadal Global Forcing for Ocean and Sea-Ice Models: The Data Sets and Flux Climatologies," Technical Report TN-460+STR, NCAR (2004).
17. V. I. Kuzin, *Method of Finite Elements in Simulating Oceanic Processes* (VTs SO AN SSSR, Novosibirsk, 1985) [in Russian].
18. E. N. Golubeva, Yu. A. Ivanov, V. I. Kuzin, and G. A. Platov, "Numerical Simulation of the World Ocean Circulation with Consideration for the Upper Quasi-Homogeneous Layer," *Okeanologiya* **32**, 395–405 (1992).
19. E. N. Golubeva, "On the Numerical Modeling of the World Ocean Circulation in the Sigma Coordinate System," *NCC Bull./Series Num. Model. Atmos. Ocean Environ. Studies* **7**, 1–7 (2001).
20. E. N. Golubeva and G. A. Platov, "On Improving the Simulation of Atlantic Water Circulation in the Arctic Ocean," *J. Geophys. Res.* **112**, doi: 10.1029/2006JC003734, C04S05 (2007).
21. E. N. Golubeva, "Numerical Simulation of the Dynamics of Atlantic Waters in the Arctic Basin with the Use of the QUISKEST Scheme," *Vych. Tekhnol.* **13** (5), 11–24 (2008).
22. B. P. Leonard, "A Stable and Accurate Convective Modeling Procedure Based on Quadratic Upstream Interpolation," *Comput. Meth. Appl. Mech. Eng.* **19**, 59–98 (1979).
23. W. D. Hibler, "A Dynamic Thermodynamic Sea Ice Model," *J. Phys. Oceanogr.* **9**, 815–846 (1979).
24. E. C. Hunke and J. K. Dukowicz, "An Elastic–Viscous–Plastic Model for Ice Dynamics," *J. Phys. Oceanogr.* **27**, 1849–1867 (1997).
25. C. M. Bitz and W. H. Lipscomb, "An Energy-Conserving Thermodynamic Model of Sea Ice," *J. Geophys. Res.* **104**, 15 669–15 677 (1999).
26. W. H. Lipscomb and E. C. Hunke, "Modeling Sea Ice Transport Using Incremental Remapping," *Mon. Weather Rev.* **132**, 1341–1354 (2004).
27. R. J. Murray, "Explicit Generation of Orthogonal Grids for Ocean Models," *J. Comput. Phys.* **126**, 251–273 (1996).
28. M. Steele, R. Morley, and W. Ermold, "PHC: A Global Hydrography with a High Quality Arctic Ocean," *J. Clim.* **14**, 2079–2087 (2000).
29. C. J. Völsch, B. Fekete, and B. A. Tucker, *River Discharge Database*, Version 1.1 (RivDIS v1.0 Suppl.) (Univ. of New Hampshire, Durham, 1998).
30. J. Bjerknes, "Atlantic Air–Sea Interaction," in *Advances in Geophysics* (Academic, New York, 1964), Vol. 10, pp. 1–82.
31. V. V. Shuleikin, *Marine Physics* (Nauka, Moscow, 1083) [in Russian].
32. L. A. Mysak and S. A. Venegas, "Decadal Climate Oscillations in the Arctic: A New Feedback Loop for Atmosphere–Ice–Ocean Interactions," *Geophys. Rev. Lett.* **25**, 3607–3610 (1998).

33. R. R. Dickson, T. J. Osborn, J. W. Hurrell, et al., "The Arctic Ocean Response to the North Atlantic Oscillation," *J. Clim.* **13**, 2671–2696 (2000).
34. J. W. Hurrell, "Decadal Trends in the North Atlantic Oscillation Regional Temperatures and Precipitation," *Science*, No. 269, 676–679 (1995).
35. V. T. Timofeev, *Water Masses of the Arctic Basin* (Gidrometeoizdat, Leningrad, 1960) [in Russian].
36. A. F. Treshnikov and G. I. Baranov, *Circulation of the Waters in the Arctic Basin* (Gidrometeoizdat, Leningrad, 1972) [in Russian].
37. Z. M. Gudkovich, "Major Patterns of Ice Drift in the Central Polar Basin," in *Proceedings of the Conference on Atmosphere–Hydrosphere Interaction in the North Atlantic* (Gidrometeoizdat, Leningrad, 1961), MGG, issues 3–4 [in Russian].
38. E. G. Nikiforov and A. O. Shpaikher, *Regularities in Forming Large-Scale Oscillations of the Hydrologic Regime in the Arctic Ocean* (Gidrometeoizdat, Leningrad, 1980) [in Russian].
39. A. Y. Proshutinsky and M. Johnson, "Two Circulation Regimes of the Wind-Driven Arctic Ocean," *J. Geophys. Res. C* **102**, 12 493–12 504 (1997).
40. A. Proshutinsky, R. H. Bourke, and F. A. McLaughlin, "The Role of the Beaufort Gyre in Arctic Climate Variability: Seasonal to Decadal Climate Scales," *Geophys. Rev. Lett.* **29**, doi: 10.1029/2002GL015847, 2100 (2000).
41. S. Hakkinen and A. Proshutinsky, "Freshwater Content Variability in the Arctic Ocean," *J. Geophys. Res.* **109**, doi: 10.1029/2003JC001940, C03051 (2004).
42. J. H. Swift, K. Aagaard, L. Timokhov, et al., "Long-Term Variability of Arctic Ocean Waters: Evidence from a Reanalysis of the EEWG Data Set," *J. Geophys. Res.* **110**, doi: 10.1029/2004JC002312 (2005).
43. M. Karcher, R. Gerdes, F. Kauker, et al., "Arctic Warming–Evolution and Spreading of the 1990s Warm Event in the Nordic Seas and in the Arctic Ocean," *J. Geophys. Res.* **108**, doi: 10.11029/2001JC002624 (2003).
44. P. Kinney, M. E. Arhelger, and D. C. Burrell, "Chemical Characteristics of Water Masses in the Amerasian Basin of the Arctic Ocean," *J. Geophys. Res.* **75**, 4097–4104 (1970).
45. R. M. Moore, M. G. Lowings, and F. C. Tan, "Geochemical Profiles in the Central Arctic Ocean: Their Relation to Freezing and Shallow Circulation," *J. Geophys. Res. C* **88**, 2667–2674 (1983).
46. L. G. Anderson, G. Bjork, O. Holby, et al., "Water Masses and Circulation in the Eurasian Basin: Results from the Oden 91 Expedition," *J. Geophys. Res. C* **99**, 3273–3283 (1994).
47. F. A. McLaughlin, E. C. Carmack, R. W. Macdonald, et al., "Physical and Geochemical Properties across the Atlantic/Pacific Water Mass Front in the Southern Canadian Basin," *J. Geophys. Res. C* **101**, 1183–1197 (1996).
48. F. A. McLaughlin, E. C. Carmack, R. W. Macdonald, et al., "The Canada Basin 1989–1995: Upstream Events and Far-Field Effects of the Barents Sea Branch," *J. Geophys. Res.* **107**, doi: 10.1029/2001JC000904, 3082 (2002).
49. W. Maslowski, B. Newton, P. Schlosser, et al., "Modeling Recent Climate Variability in the Arctic Ocean," *Geophys. Rev. Lett.* **27**, 3743–3746 (2000).